



THE UNIVERSITY *of* EDINBURGH

Edinburgh Research Explorer

Photo-ionization and fragmentation of Sc₃N@C₈₀ following excitation above the Sc K-edge

Citation for published version:

Obaid, R, Schnorr, K, Wolf, TJA, Takanashi, T, Kling, NG, Kooser, K, Nagaya, K, Wada, S, Fang, L, Augustin, S, You, D, Campbell, EEB, Fukuzawa, H, Schulz, CP, Ueda, K, Lablanquie, P, Pfeifer, T, Kukk, E & Berrah, N 2019, 'Photo-ionization and fragmentation of Sc₃N@C₈₀ following excitation above the Sc K-edge', *The Journal of Chemical Physics*, vol. 151, no. 10, pp. 104308. <https://doi.org/10.1063/1.5110297>

Digital Object Identifier (DOI):

[10.1063/1.5110297](https://doi.org/10.1063/1.5110297)

Link:

[Link to publication record in Edinburgh Research Explorer](#)

Document Version:

Peer reviewed version

Published In:

The Journal of Chemical Physics

General rights

Copyright for the publications made accessible via the Edinburgh Research Explorer is retained by the author(s) and / or other copyright owners and it is a condition of accessing these publications that users recognise and abide by the legal requirements associated with these rights.

Take down policy

The University of Edinburgh has made every reasonable effort to ensure that Edinburgh Research Explorer content complies with UK legislation. If you believe that the public display of this file breaches copyright please contact openaccess@ed.ac.uk providing details, and we will remove access to the work immediately and investigate your claim.



Photo-ionization and fragmentation of $\text{Sc}_3\text{N@C}_{80}$ following excitation above the Sc

K-edge

Razib Obaid,^{1, a)} Kirsten Schnorr,² Thomas J. A. Wolf,³ Tsukasa Takanashi,⁴ Nora
G. Kling,¹ Kuno Kooser,^{5, 6} Kiyonobu Nagaya,^{7, 8} Shin-ichi Wada,⁹ Li Fang,¹⁰
Sven Augustin,² Daehyun You,⁴ Eleanor E. B. Campbell,¹¹ Hironobu Fukuzawa,^{4, 8}
Claus-Peter Schulz,¹² Kiyoshi Ueda,^{4, 8} Pascal Lablanquie,¹³ Thomas Pfeifer,² Edwin
Kukk,⁵ and Nora Berrah¹

¹⁾*Department of Physics, University of Connecticut, USA*

²⁾*Max-Planck-Institut für Kernphysik, Germany*

³⁾*PULSE Institute, SLAC National Accelerator Laboratory,
USA*

⁴⁾*Institute of Multidisciplinary Research for Advanced Materials, Tohoku University,
Japan*

⁵⁾*Department of Physics, University of Turku, Finland*

⁶⁾*Institute of Physics, University of Tartu, Estonia*

⁷⁾*Department of Physics, Kyoto University, Japan*

⁸⁾*RIKEN SPring-8 Center, Japan*

⁹⁾*Department of Physical Science, Hiroshima University, Japan*

¹⁰⁾*Department of Physics, The Ohio State University, USA*

¹¹⁾*EastCHEM and School of Chemistry, University of Edinburgh,
United Kingdom*

¹²⁾*Max-Born-Institut, Germany*

¹³⁾*Laboratoire de Chimie Physique-Matière et Rayonnement, Sorbonne Université,
France*

We have investigated the ionization and fragmentation of a metallo-endohedral fullerene, $\text{Sc}_3\text{N@C}_{80}$ using ultrashort (10 fs) x-ray pulses. Following selective ionization of a Sc (1s) electron ($h\nu = 4.55$ keV), an Auger cascade leads predominantly to either a vibrationally cold multiply charged parent molecule or multi-fragmentation of the carbon cage following a phase transition. In contrast to previous studies, no intermediate regime of C_2 evaporation from the carbon cage is observed. A time-delayed, hard x-ray pulse ($h\nu = 5.0$ keV) was used to attempt to probe the electron transfer dynamics between the encapsulated Sc species and the carbon cage. A small but significant change in the intensity of Sc-containing fragment ions and coincidence counts for a delay of 100 fs compared to 0 fs, as well as an increase in the yield of small carbon fragment ions, may be indicative of incomplete charge transfer from the carbon cage on the sub-100 fs timescale.

^{a)}Electronic mail: razib.obaid@uconn.edu

INTRODUCTION

Endohedral (or internally doped) fullerenes, are intriguing systems that bridge the gap between molecular and nano-systems^{1,2}. Like C₆₀, there is much to learn about their behavior when they are excited with photons, in particular in the hard x-ray regime. Endohedral fullerenes are of great interest to study due to their unique properties, including electron transfer between the engaged species and the carbon cage², and their potential use in molecular electronics and organic photovoltaics. The understanding derived from the photoionization of carbon nanomaterials can provide insight towards optimizing their properties for use in these applications³. Endohedral fullerenes have been studied with optical lasers^{4,5} and synchrotron radiation⁶⁻⁹. Synchrotron studies, which allow for core-level ionization of the encapsulated species, have indicated that there is a much higher fragmentation propensity if the inner species becomes highly excited⁷, especially compared to the level of fragmentation observed following excitation/ionization of valence electrons by optical lasers⁵. The most intriguing aspect of the endohedral systems compared to empty fullerenes is the mutual influence of the electrons from the cage and the electrons from the encapsulated moiety, which may significantly modify the dynamics¹⁰.

Like synchrotron radiation, x-ray free electron lasers (FEL) can access the core levels of the inner moiety of the endohedral fullerene¹¹. The brilliance and photon energy tunability of the FEL allows for site-specific photon absorption, and because they have short pulse durations, also allows, in principle, for following the dynamics of the molecule^{11,12}. Most of the early experiments involving FELs have been on understanding the nature of the interaction of light atoms, such as neon¹³, and small molecules, such as N₂^{14,15}. Recently, polyatomic molecules¹² and fullerenes¹⁶ have been studied, with an emphasis on understanding the ionization dynamics involved when multiple x-rays are absorbed causing ionization and subsequent Auger decay, which contribute substantially to what is known as ‘radiation damage’¹⁷.

The aim of the present experiment was to investigate Sc₃N@C₈₀ by site-selectively ionizing the Sc (1s) with an approximately 10 fs duration hard x-ray pulse at 4.55 keV photon energy inducing core-ionization followed by an Auger cascade. This investigation allows us to address how electronic rearrangement affects (i) the nuclear motion leading to atomic rearrangement, (ii) bond elongation and breaking, (iii) fragmentation of the moiety (inner species) and the cage, and (iv) bond (re)-forming. For Sc, it is known that for a K-shell vacancy, the radiative to non-radiative branching ratio is 0.18:0.82, while for the L-shell vacancy, the radiative yield is negligible com-

54 expected to non-radiative relaxation which primarily occurs via Coster-Kronig type decay through
57 the LMM process¹⁸. Thus, following removal of a K-shell electron of Sc, further ionization of
58 the whole system is expected to proceed via Auger cascade or impact ionization of the cage. It is
59 expected from the binding energy of the electrons in Sc, that KLL ($2s^{-2}/2s^{-1}2p^{-1}/2p^{-2}$) Auger
60 decay will produce a free electron having a kinetic energy (KE) of about 3.5 - 4.0 keV. Likewise,
61 LMM ($3s^{-1}3p^{-1}/3p^{-2}$) decay creates $\sim 330 - 400$ eV electrons¹⁹. The high energy electrons are
62 expected to escape the cage with a low probability for further excitation of the molecule, while the
63 few-hundred eV electrons are expected to have a higher probability to undergo inelastic collisions
64 with the cage^{20,21}. A cartoon schematic of this mechanism is shown in Fig. 1 (a). We aimed to
65 study transient structural changes by using a delayed second x-ray probe pulse, at a photon energy
66 of 5.0 keV, through monitoring the production of fragment ions.

67 II. EXPERIMENT

68 The experiment was carried out at beamline BL3, EH4c hutch²² of the SPring-8 Angstrom
69 Compact free electron LAser (SACLA)²³ using a time-of-flight ion spectrometer²⁴. Both the
70 "pump" and the "probe" pulses were produced by the same electron bunch using a variable length
71 undulator scheme²⁵. For this experiment, a pump pulse with 4.55 keV photon energy (FWHM =
72 13.11 eV) and a probe pulse with 5.0 keV photon energy (FWHM = 69.79 eV) were used. Since
73 the Sc atoms have an average charge state of 2.4+ in the endohedral complex, the pump pulse was
74 tuned to be well above the K-edge of Sc (4492.8 eV²⁶), so that Sc^{3+} could be ionized by single
75 photon absorption. Meanwhile, the probe pulse was chosen to be about 5.0 keV for two reasons:
76 1) the photon energy of 5.0 keV sufficiently allows for ionization to highly charge states, above
77 4+, and 2) the difference in photon energies between the two pulses needed to be large enough
78 such that the pump and the probe could be monitored independently by an in-line spectrometer²⁷.
79 Both beams were focused by a Kirkpatrick-Baez (KB) mirror system to a focal spot size of about
80 $1.7 \times 1.8 \mu\text{m}^2$ (FWHM). Just prior to the experiment, the beam sizes were individually measured
81 by using an edge scanning method that utilizes a 200 μm gold wire to create an intensity profile²⁸.
82 During the experiment, the spatial overlap of the pump and the probe was checked for the two
83 delay points by using another 200 μm gold wire at the interaction region, since the scheme²⁵ used
84 for the production of the pump and the probe pulses did not guarantee automatic spatial overlap
85 following changes in the undulator gap of the electron bunch. The repetition rate of the pulses was

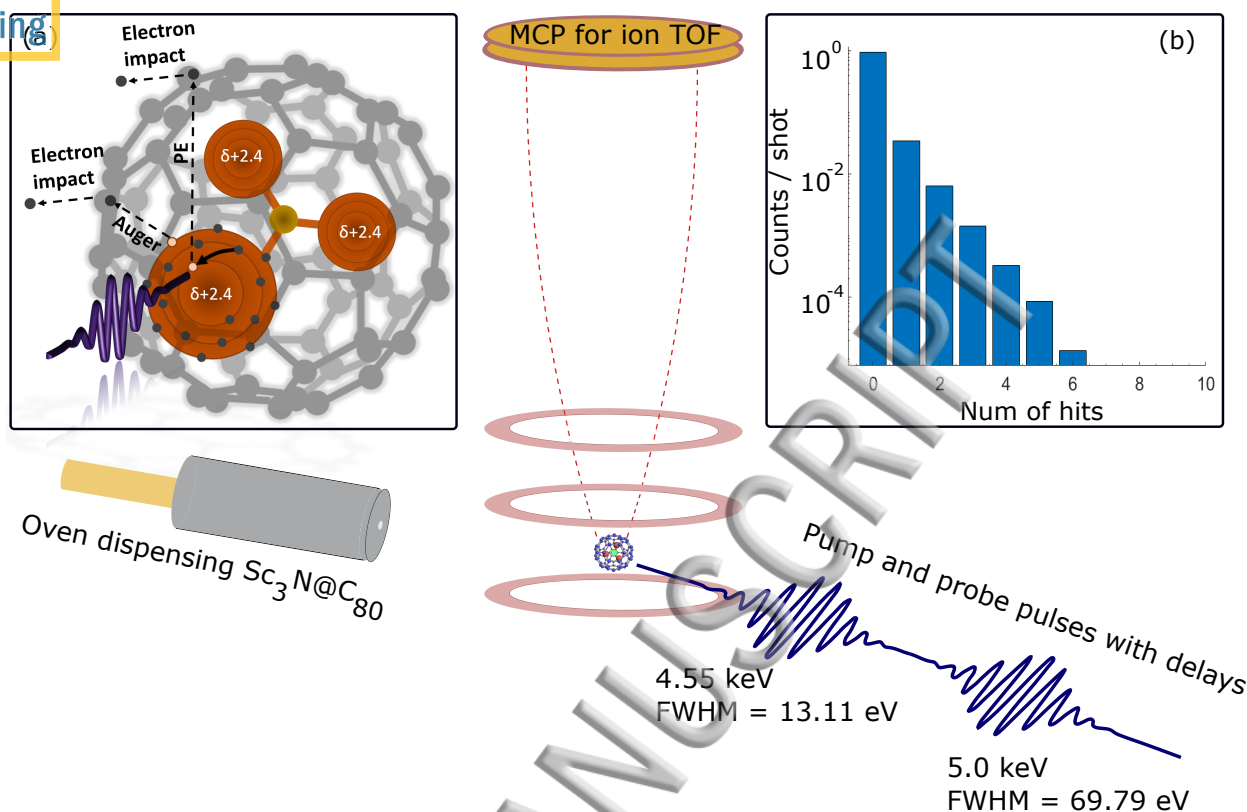


FIG. 1. Schematic of the experiment. An oven is used to vaporize the $\text{Sc}_3\text{N@C}_{80}$ sample, which is directed to the interaction region through a nozzle. The low-density molecular beam is crossed by the focused FEL pulses in the center of a time-of-flight spectrometer. A moderate extraction field applied to the spectrometer electrodes directs ions to an MCP detector. In inset (a), a cartoon of the electron impact ionization of the cage is shown following the removal of a 1s electron (photoelectron, PE) from Sc by the x-ray photon. Inset (b) shows the number of ion hits on the MCP at 100 fs delay (note that a similar hit rate is also observed for 0 fs delay).

60 Hz, and the duration of these two pulses were estimated to be about 10 fs each, as measured using a spectrometer consisting of an analyzer flat crystal of silicon²⁹ prior to the experiment. Since these measurements require their own chamber, the pulse duration was measured ex situ before the beamtime. The temporal jitter between the two pulses was estimated to be a few fs due to the electron bunch spacing, as measured previously for this scheme²⁵. Using an in-line spectrometer²⁷, the shot-to-shot pulse energy was monitored to be about 105 μJ for the pump and 110 μJ for the probe, and the energy fluctuation between the two pulses were found to be about 20% of the mean for each arm, as also shown in Fig. S1.

The experimental setup is shown schematically in Fig. 1. The $\text{Sc}_3\text{N@C}_{80}$ sample (97% purity) was procured from SES Research. The sample was converted to an effusive vapor by using a sample dispenser oven¹⁶ which evaporated $\text{Sc}_3\text{N@C}_{80}$ into its vapor phase at 970 - 1000 K. The orientation of the oven was horizontal with respect to the spectrometer axis, and along the polarization of the x-ray pulses. We estimate the target density from the oven to be about $2 \times 10^8 \text{ cm}^{-3}$.

The ions created were extracted by a uniform electric field of 550 V/cm at the interaction region, and were subsequently detected on a microchannel plate (MCP) detector. The ion hits on the MCP were recorded using a digitizer and a software discriminator³⁰. More details of the ion TOF spectrometer are described in detail elsewhere, see²⁴.

III. RESULTS AND DISCUSSION

At a fluence of about $40 \mu\text{J}/\mu\text{m}^2$ for each pulse (corresponding to an intensity of about $4 \times 10^{17} \text{ W/cm}^2$), the ionization mechanism is expected to be step-wise. First there is a photoionization (P) event followed by an intra-atomic Auger (A) decay until a stable charge state is reached. This mechanism was previously reported for FEL interactions with atoms, molecules, viruses and weakly bound clusters^{11-14,16,31-37}. At the photon energies used in the experiments, the absorption cross-section of the three scandium ions inside the cage is about $2.0 \times 10^{-19} \text{ cm}^2$ (0.2 Mb) for the 4.55 keV pump and $1.5 \times 10^{-19} \text{ cm}^2$ (0.15 Mb) for the 5.0 keV probe pulse. For the cage itself, with 80 carbon atoms, the cross-section is about $3.0 \times 10^{-20} \text{ cm}^2$ (0.03 Mb) for both of the pulses. The stability of the $\text{Sc}_3\text{N@C}_{80}$ molecular complex depends on the oxidation state of the cage. It has been determined that electron sharing with the Sc_3N stabilizes the C_{80} cage, which attains the stable icosahedral form by accepting about 6.3 electrons from the inner moiety³⁸. This induces a partial charge of 2.4+ on each Sc atom inside the cage, for the overall neutral $\text{Sc}_3\text{N@C}_{80}$.

Fig. 2 (a) shows the time-of-flight spectrum for $\text{Sc}_3\text{N@C}_{80}$, for 0 fs delay between the two x-ray pulses, with the different charge states of the parent molecular ions indicated. Multiple charge states of the parent molecule up to 4+ are observed, as seen previously for the case of the single photon ionization of the Sc 2*p* orbital⁶ for the same target. The lack of singly-charged parent molecules shows that the Sc (1*s*) photo-ionization plus Auger decay efficiently produces multiple charge states of $\text{Sc}_3\text{N@C}_{80}$. It is striking that there is no evidence in the mass spectrum for the occurrence of C_2 fragmentation from the carbon cage, i.e. $\text{Sc}_3\text{N@C}_{78}$, $\text{Sc}_3\text{N@C}_{76}$ and

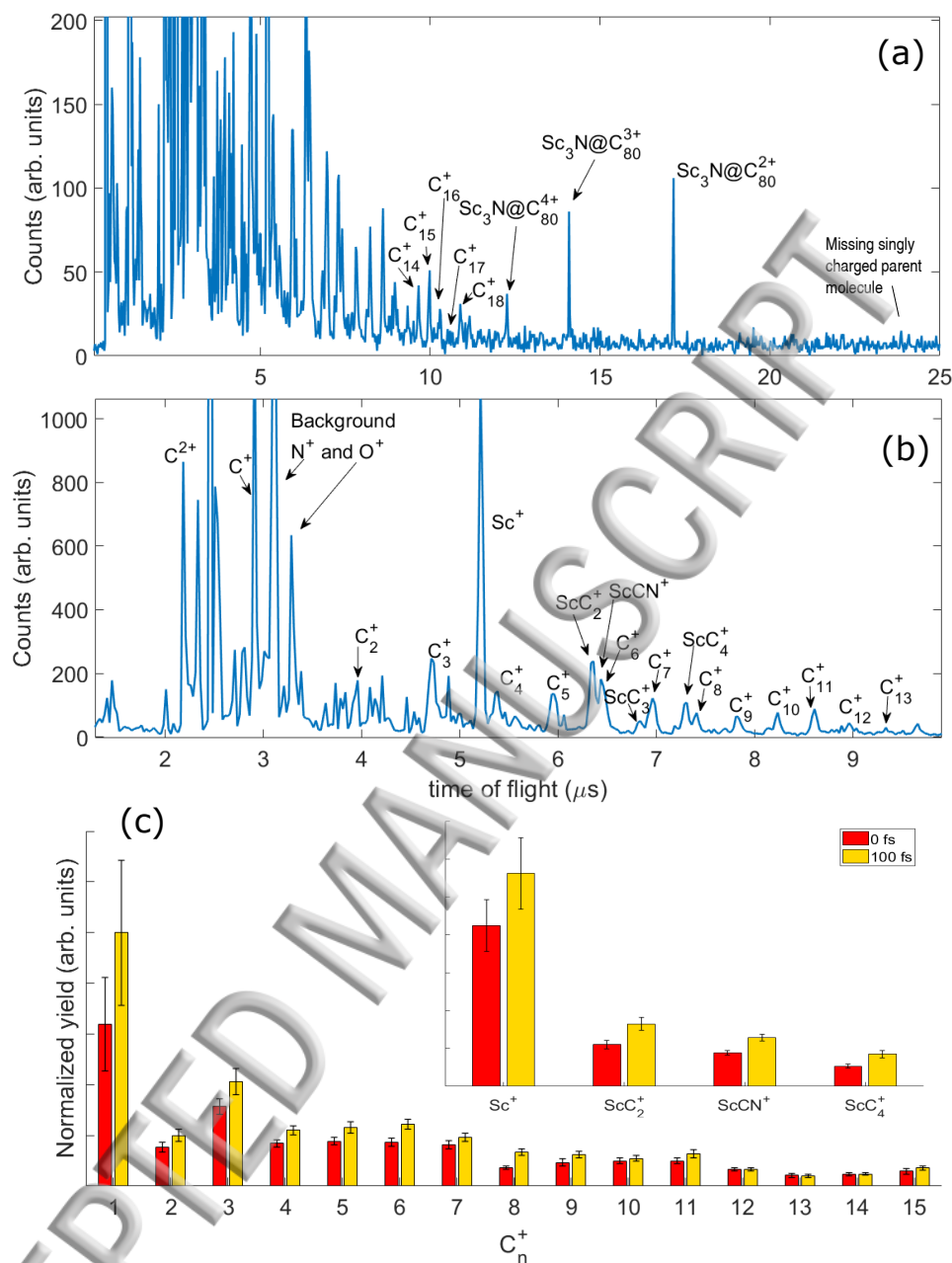


FIG. 2. Time-of-flight mass spectra for $\text{Sc}_3\text{N@C}_{80}$ with 0 fs delay between the pump and probe pulses. (a) Overall spectra highlighting the different charge states of the parent molecule as well as different fragments. (b) Zoomed-in spectrum highlighting the smaller carbon cage fragment ions. (c) Yield, normalized by the number of FEL shots and pulse energies, comparing the production of carbon fragments for 0 and 100 fs delays. The inset in (c) shows the normalized yield comparison for the Sc-containing fragments.

so on. Such typical "shrink-wrapping" behavior has been observed in previous studies where the Sc 2p orbital was photoionized⁶ and also in intense fs laser studies of $\text{Ho}_3\text{N@C}_{80}$ ⁵. The lack

of C_2 fragmentation from the cage is a clear indication that the parent molecular ions visible in the mass spectrum have low internal energies. Note that the MCP detector was not floated in these experiments to provide high impact velocity, and thus the detection efficiency of the parent molecular ions is expected to be significantly lower than that for the small carbon species in the experiments. The other striking observation is the lack of highly charged fragment ions. The highest fragment charge state that can be clearly distinguished in the spectra is C^{2+} with possibly a small amount of Sc^{2+} . The low level of charging and corresponding lack of Coulomb explosion is also manifested by the rather narrow ion peaks and the dominance of the detection of single ions per shot (ca. 96 % of all shots that yield an ion signal), as illustrated in Fig. 1 (b). The most stable charge on the parent molecule is 2+ and 3+. This may be due to the stabilizing nature of the π electron delocalization in the system following ionization, which corresponds to a larger gap between the HOMO and LUMO orbital for the resultant multiply charged parent molecule³⁹. Fig. 2 (b) shows the time-of-flight spectrum for the various singly-charged carbon fragments. We observe carbon fragments, C_n^+ for $n < 20$. Some doubly charged atomic carbon is also observed, indicating that a portion of the carbon atoms in the cage lost multiple electrons either through their transfer from the cage to the moiety, or through electron collisions from the Auger electrons. What is surprisingly missing in the time-of-flight spectra is the observation of highly charged ($>2+$) states of Sc ions which one may have expected following Sc (1s) photo-ionization and subsequent Auger decay. That we mainly observe Sc^+ , and only a small amount of Sc^{2+} , seems to be indicative of charge being efficiently transferred from the cage to the Sc ions.

In Fig. 2 (c), we show the yield of the singly charged carbon fragments for the two delay points, normalized to the number of shots and pulse energy per shot (see supplemental information figure S1 for the distribution of pulse energies for the two pump-probe experiments). The inset shows the Sc-containing fragment ion yields, which includes Sc^+ , ScC_2^+ , $ScCN^+$, and ScC_4^+ . The latter three fragments are products requiring new bond formation since in the initial system, no direct bond existed between the three Sc and the C_{80} cage. Such new bonds are typically observed following ionization and multi-fragmentation of the cage, as seen previously for the case of FEL and fs optical laser-induced fragmentation of $Ho_3N@C_{80}$ ^{5,32} as well as photo-ionization of Sc (2p) in $Sc_3N@C_{80}$ ⁶ and intense ns optical laser photoionization/fragmentation of $La@C_{82}$ ⁴. On comparison of the two sets of data, the normalized ion yield is slightly higher for the small carbon species and, more significantly, the scandium-containing small fragments at 100 fs delay compared to 0 fs. Due to technical reasons of the two pulse scheme²⁵, the only way single pulse spectra could be

obtained is by filtering out the probe pulse using an Al filter. This resulted in some absorption of the pump pulse, and thus the pulse energy for single pulse mode was different than what was used for the two pulse experiment. Single pulse spectra obtained for pulse energies of 80 μJ and 520 μJ show mostly similar trends in the relative intensities of the fragment ion peaks (see supplemental information figures S2, S3, and S4). The pulse energy variation between the two delays (0 fs and 100 fs) was about 5%, which should not change the fact that what we are seeing is predominantly single photon absorption (see supplemental information figure S5, which shows that the effect of this pulse energy variation is negligible for multiple ionization of parent molecules). Inside the cage, each Sc has contributed about 3 electrons to the cage and the nitrogen atom. This implies that the 3d and 4s levels are not occupied. The x-ray absorption first leads to a KLL process, leaving two L-shell holes. This can be followed by subsequent decay of two M-shell electrons to fill the holes. Since direct double ionization has a much lower probability than single Auger decay⁴⁰, this would leave the system with the 4 electrons removed from the Sc. Electrons from the cage would then flow to the ionized Sc. If very little energy is transferred to the cage on the way out or via the charge rearrangement process then one could expect to see up to $\text{Sc}_3\text{N}@\text{C}_{80}^{4+}$. If the system absorbed more than one photon, then we would expect to see higher charge states. However, the stability of endohedral fullerenes is also dependent upon the π -orbital delocalization of the system³⁹, and does not support high charge states beyond 5+. For the case of single photon absorption, one can definitely create multiple charge states on the Sc site. However, as also observed in previous studies of Sc $2p$ ionization⁶, competing processes of cascade ionization and charge rearrangement from the cage to the moiety leads to fragmentation, as it becomes more and more unfavorable for the system to remain stable with increasingly higher charge states. Therefore, further ionization of the cage would result in instability of the system, manifested by cage opening/break up. This ensures that the products which will show time-dependent features are fragments ensuing from charge rearrangements by the cage. Such fragments are Sc^+ , ScCN^+ , ScC_2^+ , ScC_3^+ , and so on. It is expected that if the two photon processes are initiated by the absorption of the pump and the probe pulses by the same system, then the newly formed ScC_n^+ would further ionize and fragment.

In the present case, differences between the two delay points include a significant non-linear increase of the C_3^+ intensity relative to the other small carbon species and the Sc^+ intensity relative to the other Sc-containing fragments at the higher pulse energy, which may be indicative of 2-photon processes. In order to obtain more evidence for this we consider the ions that are detected

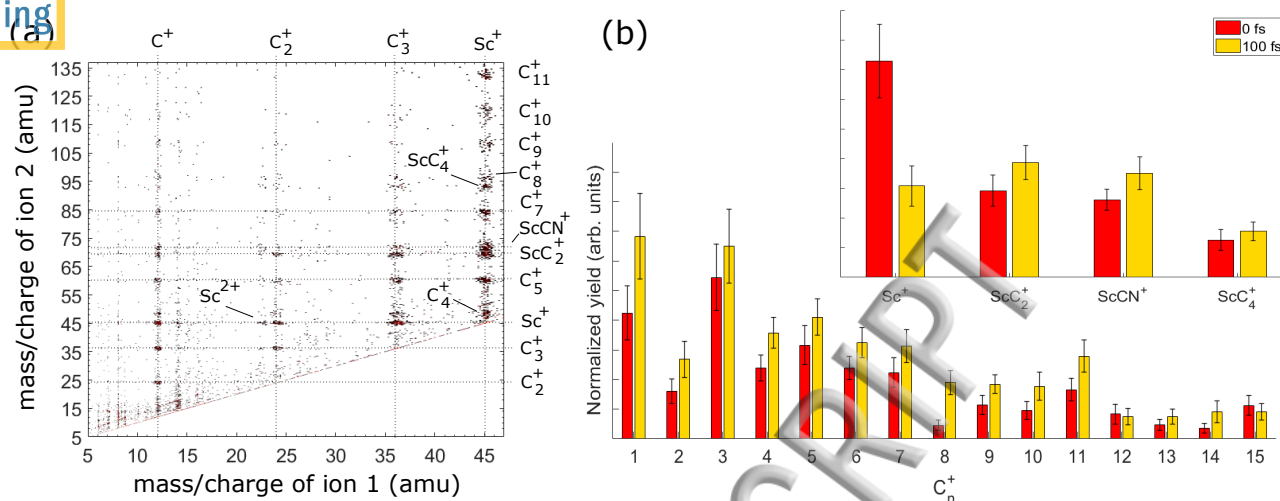


FIG. 3. (a) Photo-ion photo-ion coincidence map at the pump-probe delay of 100 fs. The mass/charge ratio is derived directly from the time-of-flight. Ions 1 and 2 are the first and second ions to hit the detector for a given FEL shot. (b) The yield corresponding to the two pump-probe delays for different carbon fragments coincident with the detection of Sc^+ . The inset in (b) shows the yield for species produced due to a newly formed bond between the Sc ions and fragments originating from the carbon cage. In both cases for (b), the yield is normalized by the number of FEL shots for the two pump-probe delays. Note that Fig 2 (c) and insets are plotted on the same scale as (b).

in coincidence.

Fig. 3 (a) shows a portion of the photo-ion photo-ion coincidence (pipico) map for ions relevant to Sc^+ and small carbon fragment ions. Since the MCP detector count rate was $\ll 1/\text{shot}$ (about 5% of the FEL shot produced any hits on the MCP for the two pulses), we assume the ions coincident with each other evolved from the same molecule. The prominent partner ions detected in coincidence with Sc^+ are C_n^+ with n spanning $n = 1 - 18$. Note that it is not possible to rule out the contribution of doubly or triply charged species with the same mass/charge ratio as the singly charged species. However a consideration of the peak shapes in the mass spectra would indicate that the contribution of multiply-charged species is very low.

In Fig. 3 (b), we also see a larger intensity for coincidences between Sc^+ and C_n^+ for the 100 fs delay data, particularly for the smallest carbon species. There is a more obvious difference in the coincidences between Sc^+ and scandium-containing fragment ions with a very significant decrease in the $\text{Sc}^+ - \text{Sc}^+$ coincidence rate for a delay of 100 fs and increase in the $\text{Sc}^+ - \text{ScC}_2^+$ and $\text{Sc}^+ - \text{ScCN}^+$ intensities. From the pipico data, we also observe indications of Sc^{2+} coincident with Sc^+ ,

with the prominent cage fragment C_3^+ , and with ions where pieces of the cage have formed new bonds with atoms originating inside the cage, i.e. ScC_2^+ and $ScCN^+$. As there are large neutral fragments from the original molecule not accounted for, these pipico structures do not form sharp lines, but rather small blobs, as long as the remaining fragment(s) do not carry the majority of the dissociation momentum. Somewhat surprisingly, we do not observe a noticeable amount of Sc^{2+} coincident with species other than Sc^+ , although we also expect these coincidences to be difficult to identify due to the higher level of multi-body fragmentation, further blurring out the ion-ion coincidence islands. There are also some indications of carbon fragment ions being produced in coincidence with other carbon fragment ions, such as $C^+ + C_2^+$, $C^+ + C_3^+$, $C^+ + C_4^+$, $C^+ + C_5^+$, $C^+ + C_7^+$ and others.

A consideration of both the full mass spectra and the coincidence data allows us to draw some interesting conclusions about the ionization and fragmentation behavior of the $Sc_3N@C_{80}$ molecule. The full mass spectra, that we believe to be dominated by single-photon absorption, provide evidence for two distinct processes. Firstly, the strong signal from intact parent molecular ions with charge states from 2+ to 4+ is indicative of Auger cascades involving predominantly the Sc. The doubly charged species arises from a single KLL Auger transition from the Sc (2p) with the emission of a high energy electron. **If we consider the role of the cage which encapsulates the moiety, then we would see that C_{80}^{4-} , which is the charge state of the cage after charge rearrangement followed by removal of 2 electrons from a single Sc, is as stable as C_{80}^{6-} , which is the charge states attained by the cage in the neutral system³⁹. This is analogous to stating that $Sc_3N@C_{80}^{2+}$ is as stable as the neutral system due to the interplay of the charge stabilization by the π orbital and the strain effect due to Coulomb repulsion.** Triply and quadruply charged species most likely arise from LMM Auger decays within Sc. Considering that, within the cage, Sc exists on average in a 2.4+ charge state, no further Auger decays within the Sc system to produce higher charge states are possible. For the highest observable charge state, this would leave a Sc ion with an electron configuration of $1s^2 2s^2 2p^4 3s^2 3p^6$. Any subsequent re-arrangement of electrons within the endohedral fullerene system to compensate for the high charge on the Sc ion would transfer electrons either from neighboring species inside the cage or from the carbon atoms in the cage. The lack of C_2 evaporation from these parent molecular ion species, such as $Sc_3N@C_{78}$, $Sc_3N@C_{76}$ and so on, (see Fig. 2 (a)) is a clear indication that energy transferred to internal vibrational energy of the cage is insufficient to produce any fragmentation on the microsecond timescale in which the ions reside in the extraction region of the mass spectrometer. This would be expected for sequential

transfer of electrons from the carbon cage to the Sc ($n = 3$) shell. It can therefore be assumed that to produce these intact parent molecular ions, the energetic electrons emitted from the KLL and LMM cascades do not collide inelastically with the carbon cage while exiting the molecule. If however, there is an inelastic collision between the 300-400 eV electrons from the LMM cascades with the carbon cage, this will provide enough internal excitation to induce a phase transition in the hot molecule⁴¹ leading to rapid cage break-up and the characteristic mass spectrum of small carbon fragment ions that we observe. Extensively studied fragmentation patterns using multiphoton laser excitation⁴² or collisional excitation⁴³ transfer a wide range of energies to the fullerenes and typically produce a bimodal fragment distribution. Here, we either transfer sufficient energy via inelastic transfer of energy from electrons produced within the cage to cause rapid statistical cage break-up and the formation of singly-charged ring and chain fragments or there is insufficient energy transferred to evaporate C_2 from the cage on the timescale of the mass spectrometry detection, leaving intact parent molecular ions.

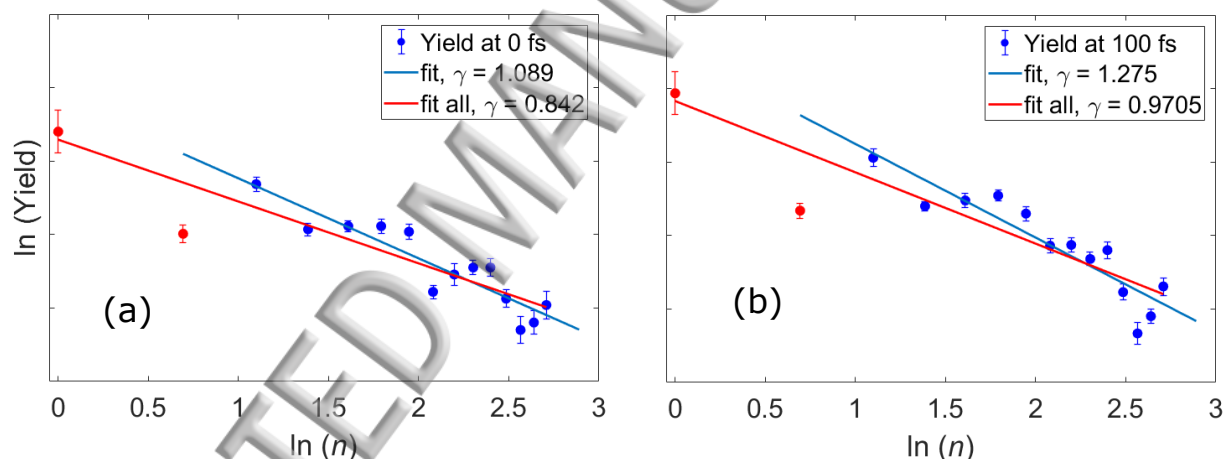


FIG. 4. Logarithmic total yields of C_n^+ for (a) 0 fs and (b) 100 fs. In both panels the blue lines show the linear fits considering fragments C_3^+ to C_{15}^+ , with the first two carbon fragments (C^+ and C_2^+) excluded (shown as red dots). In (a) and (b), the red lines show the linear fits considering all the carbon fragments.

Both graphs have the same scale.

The statistical break-up of internally excited fullerene cages had been modeled previously using both a percolation model⁴⁴ and a maximum entropy model⁴¹. In the bond percolation model, a power-law distribution for the small cage fragment species is predicted. The fragment ion intensities for both the 0 fs and 100 fs delay data have been plotted on a ln-ln plot in Fig. 4. Figures 4 (a) and (b) show that the data fits reasonably well to the expected power law behavior for all

fragments from C_3^+ to C_{15}^+ , as given by: $S_n \propto n^{-\gamma}$. Here S_n is the yield of carbon fragments, C_n^+ , and n is the number of carbon atoms, while γ is the fit parameter. The goodness of the fit, R^2 , for the blue fit lines for Fig. 4 (a) and (b) are 0.63, 0.82 respectively. For the fragmentation of a cage system such as C_{60} , it has been shown previously that due to finiteness and the periodic nature of the system, $\gamma \approx 1.3$ is obtained for a fullerene system undergoing a phase transition by emitting small carbon molecular fragments⁴⁴. This value of γ is a consequence of the amount of energy transferred to the fullerene in the highly charged ion collisions⁴⁴ after averaging over the impact parameter dependence of the energy transfer. The gradient will change depending on how much internal energy is present in the system. For very high amounts of internal energy, γ will be higher since the fragment distribution will shift more to smaller mass ions. Since, neither from the consideration of C^+ and C_2^+ nor from their omission in the overall ln-ln fit, we did not obtain value of γ higher than 1.3 for any of the delays, it can be said that the measured distribution is consistent with the power law behavior expected from statistical break-up as predicted by the percolation model, in analogy with nuclear multi-fragmentation^{45,46}.

The maximum entropy model as applied to C_{60} shows similar behavior but is able to reproduce variations in the relative intensities, including the lower than predicted yield for C^+ and C_2^+ by taking the ionization energies and binding energies of all possible fragments into consideration⁴¹. For C_{60} the internal energy leading to the observation of the small carbon ring and chain fragment ions was shown to be at about 230 eV⁴¹ while for the larger endohedral system $La@C_{82}$ it was predicted to be at about 300 eV⁴. A simple extrapolation based on the number of degrees of freedom for $Sc_3N@C_{80}$ would lead to an expected threshold for the phase transition of about 320 eV. A lower energy would be expected if the cage was multiply charged. This energy is consistent with the electron energies produced by the LMM Auger transitions in Sc. The observed behavior is thus supporting a model in which the cage is efficiently excited (possibly further ionized) by interaction with Auger electrons as they exit the molecule, leading to a rapid energy equilibration followed by cage break-up into predominantly singly-charged fragments. Application of the maximum entropy model to $La@C_{82}$ fragmentation was also shown to reproduce the formation of $La@C_n^+$ fragments, similar to the scandium-containing ions observed in the current experiments⁴. The statistical nature of the break-up will also discriminate against highly charged ions in the maximum entropy model due to their relatively higher ionization energies. The consideration of established results from both these models provide further support for our assertion that the single photon absorption process from the pump pulse alone initiates the cage breakup in the present

If we again turn our attention to the coincidence data in Fig. 3 (b), we see small but significant differences between the 0 fs and the 100 fs data which may be indicative of two-photon processes and the timescale of intramolecular electron transfer events. The increase in the intensity of coincidences between Sc^+ and small scandium-containing fragment ions compared to coincidences between two singly-charged scandium ions could be due to the dynamics of electron transfer from the carbon cage to the photoionized Sc ions. At 0 fs delay, all direct or Auger induced photoionization can be expected to occur on the 10 fs timescale. Any two-photon absorption is likely to produce two charged Sc species within the cage giving a relatively high probability to detect a $\text{Sc}^+ - \text{Sc}^+$ coincidence signal for 0 fs delay (taking into consideration the energy and charge equilibration that will take place as the system is undergoing the rapid phase transition and break-up). After a delay of 100 fs, there is time for electron transfer from the cage carbon atoms to the highly charged Sc to occur, transferring the positive charge to the cage prior to the absorption of the second photon, and therefore giving a higher probability to detect more small charged carbon species in coincidence with Sc^+ on the second (P)-(A) cycle. The higher yield of coincidences between Sc^+ and scandium-containing fragment ions for 100 fs delay may be caused by the initiation of the cage break-up on this timescale after the first photon absorption. In the total count of Sc^+ , as seen in Fig. 2 (c), we do not see a significant difference between the two delays. K-shell ionization of two neighboring Sc is more likely to give $\text{Sc}^+ - \text{Sc}^+$ coincidences than in the single photon case. We can see from Fig. S3 that the single pulse $\text{Sc}^+ - \text{Sc}^+$ peak is much lower in intensity than the pump-probe coincidence data in Fig. 3. This is reasonably convincing evidence that a majority of the intensity of the $\text{Sc}^+ - \text{Sc}^+$ coincidence peak in Fig. 3 is coming from the pump-probe. At 100 fs, the Fig. 3 distribution is much closer to that of Fig. S3, and we can interpret that as the holes in the first ionized Sc being refilled due to transfer from the cage on a sub-100 fs timescale, so that for a delay of 100 fs the Sc is basically similar to that of the pristine molecule with the charge transferred to the carbon cage.

IV. SUMMARY AND CONCLUSION

We have experimentally probed the photo-ionization and fragmentation behavior of $\text{Sc}_3\text{N@C}_{80}$ following K-shell core ionization of the encapsulated Sc. The mass spectra provide evidence for two processes leading to distinct signatures in the ion distributions: (i) multiple ionization of the

317 fragment molecular ion via Auger cascades that transfer sufficiently little energy to vibrational exci-
318 tation of the molecule to survive intact during the microsecond timescale of the mass spectrometer
319 and (ii) high-energy transfer to the cage followed by cage break-up and the production of small,
320 predominantly singly-charged fragment ions. Pump-probe measurements at delays of 0 fs and 100
321 fs provided additional evidence for a "slow" (> 10 fs) electron transfer between the carbon cage
322 and the multiply-ionized Sc ions. Due to the "all or nothing" nature of the energy transfer to the
323 cage, the mass spectra look quite different to the typical bimodal fragment distributions that are
324 normally observed for fragmenting fullerene species. The absence of highly charged species is also
325 an unusual feature for K-shell excitation studies and is thought to be a consequence of the particu-
326 lar geometry of the endohedral species and the highly statistical nature of fullerene fragmentation.
327 Although the current data is of a rather preliminary nature and requires further experimental and
328 theoretical study to fully unravel the complex dynamics of the studied system, we have shown
329 the feasibility of x-ray FEL pump-probe experiments to probe the complex electron and nuclear
dynamics of large molecular systems.

330 SUPPLEMENTARY MATERIAL

331 See 'Supplementary Information' for the figures S1, S2, S3, S4 and S5 mentioned in the
332 manuscript.

333 ACKNOWLEDGEMENT

334 This work was funded by the Chemical Sciences, Geosciences, and Biosciences Division,
335 Office of Basic Energy Sciences, Office of Science, U.S. Department of Energy, grant No.
336 DE-SC0012376. T. T. gratefully acknowledges support by the JSPS KAKENHI Grant Number
337 JP16J02270. H. F., K. N., and K. U. were supported by "Dynamic Alliance for Open Innovation
338 Bridging Human, Environment and Materials" from the Ministry of Education, Culture, Sports,
339 Science and Technology of Japan (MEXT), by the Research Program of "Dynamic Alliance
340 for Open Innovation Bridging Human, Environment and Materials" in "Network Joint Research
341 Center for Materials and Devices", by the Japan Society for the Promotion of Science (JSPS)
342 KAKENHI Grant Numbers JP15K17487, and by the IMRAM project. D.Y. was supported by a
343 Grant-in-Aid of Tohoku University Institute for Promoting Graduate Degree Programs Division

for Interdisciplinary Advanced Research and Education.

We would like to thank the SACLA Accelerator scientists and beamline staff for the technical and experimental help provided during the beamtime.

REFERENCES

- ¹H. Shinohara and N. Tagmatarchis, *Endohedral Metallofullerenes: Fullerenes with Metal Inside* (Wiley, 2015).
- ²A. Rodríguez-Forteza, A. L. Balch, and J. M. Poblet, “Endohedral metallofullerenes: a unique host–guest association,” *Chemical Society Reviews* **40**, 3551–3563 (2011).
- ³Y. Wang, R. Yamachika, A. Wachowiak, M. Grobis, and M. F. Crommie, “Tuning fulleride electronic structure and molecular ordering via variable layer index,” *Nature Materials* **7**, 194 (2008).
- ⁴A. Lassesson, A. Gromov, K. Mehlig, A. Taninaka, H. Shinohara, and E. E. B. Campbell, “Formation of small lanthanum–carbide ions from laser induced fragmentation of La@C_{82} ,” *The Journal of Chemical Physics* **119**, 5591–5600 (2003).
- ⁵H. Xiong, L. Fang, T. Osipov, N. G. Kling, T. J. A. Wolf, E. Sistrunk, R. Obaid, M. Gühr, and N. Berrah, “Fragmentation of endohedral fullerene $\text{Ho}_3\text{N@C}_{80}$ in an intense femtosecond near-infrared laser field,” *Physical Review A* **97**, 023419 (2018).
- ⁶H. Xiong, R. Obaid, L. Fang, C. Bomme, N. G. Kling, U. Ablikim, V. Petrovic, C. E. Liekhus-Schmaltz, H. Li, R. C. Bilodeau, *et al.*, “Soft x-ray induced ionization and fragmentation dynamics of $\text{Sc}_3\text{N@C}_{80}$ investigated using an ion-ion-coincidence momentum-imaging technique,” *Physical Review A* **96**, 033408 (2017).
- ⁷J. Hellhund, A. Borovik Jr, K. Holste, S. Klumpp, M. Martins, S. Ricz, S. Schippers, and A. Mueller, “Photoionization and photofragmentation of multiply charged $\text{Lu}_3\text{N@C}_{80}$ ions,” *Physical Review A* **92**, 013413 (2015).
- ⁸A. Müller, S. Schippers, R. A. Phaneuf, M. Habibi, D. Esteves, J. C. Wang, A. L. D. Kilcoyne, A. Aguilar, S. Yang, and L. Dunsch, “Photoionization of the endohedral fullerene ions $\text{Sc}_3\text{N@C}_{80}$ and Ce@C_{82} by synchrotron radiation,” *Journal of Physics: Conference Series* **88**, 012038 (2007).
- ⁹A. Müller, M. Martins, A. Kilcoyne, R. Phaneuf, J. Hellhund, A. Borovik Jr, K. Holste, S. Bari, T. Buhr, S. Klumpp, *et al.*, “Photoionization and photofragmentation of singly charged positive

and negative $\text{Sc}_3\text{N@C}_{80}$ endohedral fullerene ions,” *Physical Review A* **99**, 063401 (2019).

¹⁰B. Mignolet, T. Kus, and F. Remacle, “Imaging orbitals by ionization or electron attachment: The role of dyson orbitals,” in *Imaging and Manipulating Molecular Orbitals* (Springer, 2013) pp. 41–54.

¹¹N. Berrah, J. Bozek, J. Costello, S. Düsterer, L. Fang, J. Feldhaus, H. Fukuzawa, M. Hoener, Y. Jiang, P. Johnsson, *et al.*, “Non-linear processes in the interaction of atoms and molecules with intense EUV and x-ray fields from SASE free electron lasers (FELs),” *Journal of Modern Optics* **57**, 1015–1040 (2010).

¹²A. Rudenko, L. Inhester, K. Hanasaki, X. Li, S. Robatjazi, B. Erk, R. Boll, K. Toyota, Y. Hao, O. Vendrell, *et al.*, “Femtosecond response of polyatomic molecules to ultra-intense hard x-rays,” *Nature* **546**, 129 (2017).

¹³L. Young, E. Kanter, B. Krässig, Y. Li, A. March, S. Pratt, R. Santra, S. Southworth, N. Rohringer, L. DiMauro, *et al.*, “Femtosecond electronic response of atoms to ultra-intense x-rays,” *Nature* **466**, 56 (2010).

¹⁴L. Fang, M. Hoener, O. Gessner, F. Tarantelli, S. T. Pratt, O. Kornilov, C. Buth, M. Gühr, E. P. Kanter, C. Bostedt, *et al.*, “Double core-hole production in N_2 : beating the Auger clock,” *Physical Review Letters* **105**, 083005 (2010).

¹⁵M. Hoener, L. Fang, O. Kornilov, O. Gessner, S. T. Pratt, M. Gühr, E. P. Kanter, C. Blaga, C. Bostedt, J. D. Bozek, *et al.*, “Ultraintense x-ray induced ionization, dissociation, and frustrated absorption in molecular nitrogen,” *Physical Review Letters* **104**, 253002 (2010).

¹⁶B. Murphy, T. Osipov, Z. Jurek, L. Fang, S.-K. Son, M. Mucke, J. Eland, V. Zhaunerchyk, R. Feifel, L. Avaldi, *et al.*, “Femtosecond x-ray-induced explosion of C_{60} at extreme intensity,” *Nature Communications* **5**, 4281 (2014).

¹⁷B. Abbey, R. A. Dilanian, C. Darmanin, R. A. Ryan, C. T. Putkunz, A. V. Martin, D. Wood, V. Streltsov, M. W. M. Jones, N. Gaffney, F. Hofmann, G. J. Williams, S. Boutet, M. Messerschmidt, M. M. Seibert, S. Williams, E. Curwood, E. Balaur, A. G. Peele, K. A. Nugent, and H. M. Quiney, “X-ray laser-induced electron dynamics observed by femtosecond diffraction from nanocrystals of Buckminsterfullerene,” *Science Advances* **2** (2016), 10.1126/sciadv.1601186.

¹⁸M. O. Krause, “Atomic radiative and radiationless yields for K and L shells,” *Journal of Physical and Chemical Reference Data* **8**, 307–327 (1979).

¹⁹C. E. Moore and H. N. Russell, “Binding energies for electrons of different types,” *Journal of*

Research of the National Bureau of Standards **48**, 2285 (1952).

²⁰B. Dünser, M. Lezius, P. Scheier, H. Deutsch, and T. Märk, “Electron impact ionization of C₆₀,”
Physical Review Letters **74**, 3364 (1995).

²¹A. A. Vostrikov, D. Y. Dubnov, and A. A. Agarkov, “Inelastic interaction of an electron with a
C₆₀ cluster,” High Temperature **39**, 22–30 (2001).

²²M. Yabashi, H. Tanaka, and T. Ishikawa, “Overview of the SACLA facility,” Journal of Syn-
chrotron Radiation **22**, 477–484 (2015).

²³T. Ishikawa, H. Aoyagi, T. Asaka, Y. Asano, N. Azumi, T. Bizen, H. Ego, K. Fukami, T. Fukui,
Y. Furukawa, *et al.*, “A compact x-ray free-electron laser emitting in the sub-ångström region,”
Nature Photonics **6**, 540 (2012).

²⁴H. Fukuzawa, K. Nagaya, and K. Ueda, “Advances in instrumentation for gas-phase spec-
troscopy and diffraction with short-wavelength free electron lasers,” Nuclear Instruments and
Methods in Physics Research Section A: Accelerators, Spectrometers, Detectors and Associated
Equipment **907**, 116–131 (2018).

²⁵T. Hara, Y. Inubushi, T. Katayama, T. Sato, H. Tanaka, T. Tanaka, T. Togashi, K. Togawa,
K. Tono, M. Yabashi, *et al.*, “Two-colour hard x-ray free-electron laser with wide tunability,”
Nature Communications **4**, 2919 (2013).

²⁶J. A. Bearden and A. Burr, “Reevaluation of x-ray atomic energy levels,” Reviews of Modern
Physics **39**, 125 (1967).

²⁷K. Tamasaku, Y. Inubushi, I. Inoue, K. Tono, M. Yabashi, and T. Ishikawa, “Inline spectrometer
for shot-by-shot determination of pulse energies of a two-color x-ray free-electron laser,” Journal
of Synchrotron Radiation **23**, 331–333 (2016).

²⁸H. Yumoto, H. Mimura, S. Matsuyama, T. Koyama, Y. Hachisu, T. Kimura, H. Yokoyama,
J. Kim, Y. Sano, K. Tono, *et al.*, “Micro-focusing of hard x-ray free electron laser radiation
using Kirkpatrick-Baez mirror system,” in *Journal of Physics: Conference Series*, Vol. 425 (IOP
Publishing, 2013) p. 052022.

²⁹Y. Inubushi, K. Tono, T. Togashi, T. Sato, T. Hatsui, T. Kameshima, K. Togawa, T. Hara,
T. Tanaka, H. Tanaka, *et al.*, “Determination of the pulse duration of an x-ray free electron
laser using highly resolved single-shot spectra,” Physical Review Letters **109**, 144801 (2012).

³⁰K. Motomura, L. Foucar, A. Czasch, N. Saito, O. Jagutzki, H. Schmidt-Böcking, R. Dörner, X.-
J. Liu, H. Fukuzawa, G. Prümper, *et al.*, “Multi-coincidence ion detection system for EUV–FEL
fragmentation experiments at SPring-8,” Nuclear Instruments and Methods in Physics Research

Section A: Accelerators, Spectrometers, Detectors and Associated Equipment **606**, 770–773

(2009).

³¹B. Rudek, K. Toyota, L. Foucar, B. Erk, R. Boll, C. Bomme, J. Correa, S. Carron, S. Boutet, G. J. Williams, *et al.*, “Relativistic and resonant effects in the ionization of heavy atoms by ultra-intense hard x-rays,” *Nature Communications* **9**, 4200 (2018).

³²N. Berrah, B. Murphy, H. Xiong, L. Fang, T. Osipov, E. Kukk, M. Guehr, R. Feifel, V. Petrovic, K. Ferguson, *et al.*, “Femtosecond x-ray-induced fragmentation of fullerenes,” *Journal of Modern Optics* **63**, 390–401 (2016).

³³R. Obaid, C. Buth, G. L. Dakovski, R. Beerwerth, M. Holmes, J. Aldrich, M.-F. Lin, M. Minitti, T. Osipov, W. Schlotter, *et al.*, “LCLS in—photon out: fluorescence measurement of neon using soft x-rays,” *Journal of Physics B: Atomic, Molecular and Optical Physics* **51**, 034003 (2018).

³⁴T. Ekeberg, M. Svenda, C. Abergel, F. R. Maia, V. Seltzer, J.-M. Claverie, M. Hantke, O. Jönsson, C. Nettelblad, G. Van Der Schot, *et al.*, “Three-dimensional reconstruction of the giant mimivirus particle with an x-ray free-electron laser,” *Physical Review Letters* **114**, 098102 (2015).

³⁵C. Bostedt, S. Boutet, D. M. Fritz, Z. Huang, H. J. Lee, H. T. Lemke, A. Robert, W. F. Schlotter, J. J. Turner, and G. J. Williams, “Linac Coherent Light Source: The first five years,” *Reviews of Modern Physics* **88**, 015007 (2016).

³⁶N. Berrah, “A perspective for investigating photo-induced molecular dynamics from within with femtosecond free electron lasers,” *Physical Chemistry Chemical Physics* **19**, 19536–19544 (2017).

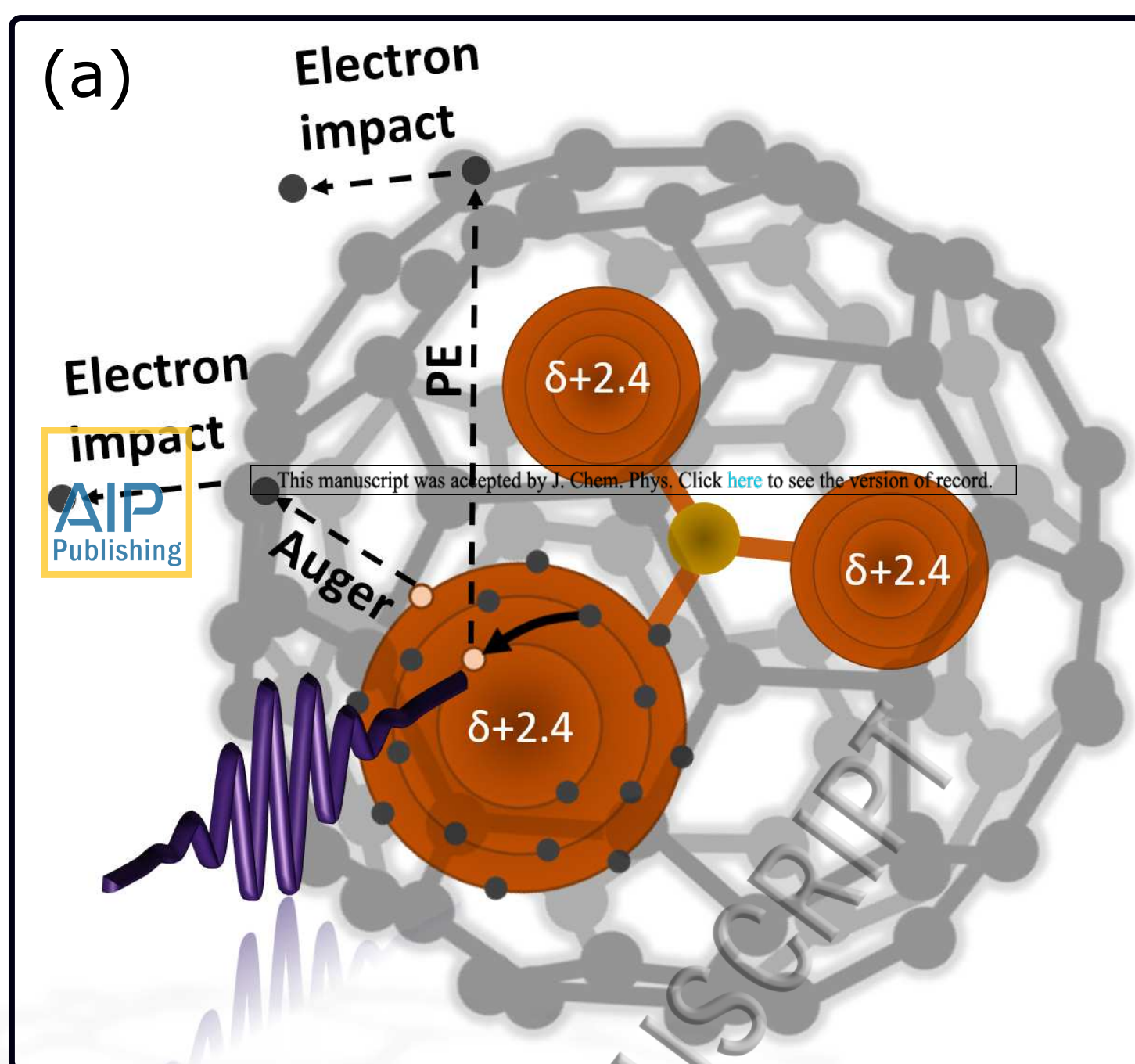
³⁷L. Young, K. Ueda, M. Gühr, P. H. Bucksbaum, M. Simon, S. Mukamel, N. Rohringer, K. C. Prince, C. Masciovecchio, M. Meyer, *et al.*, “Roadmap of ultrafast x-ray atomic and molecular physics,” *Journal of Physics B: Atomic, Molecular and Optical Physics* **51**, 032003 (2018).

³⁸L. Alvarez, T. Pichler, P. Georgi, T. Schwieger, H. Peisert, L. Dunsch, Z. Hu, M. Knupfer, J. Fink, P. Bressler, M. Mast, and M. S. Golden, “Electronic structure of pristine and intercalated Sc₃N@C₈₀ metallofullerene,” *Phys. Rev. B* **66**, 035107 (2002).

³⁹Y. Wang, S. Díaz-Tendero, M. Alcamí, and F. Martín, “Cage connectivity and frontier π orbitals govern the relative stability of charged fullerene isomers,” *Nature Chemistry* **7**, 927 (2015).

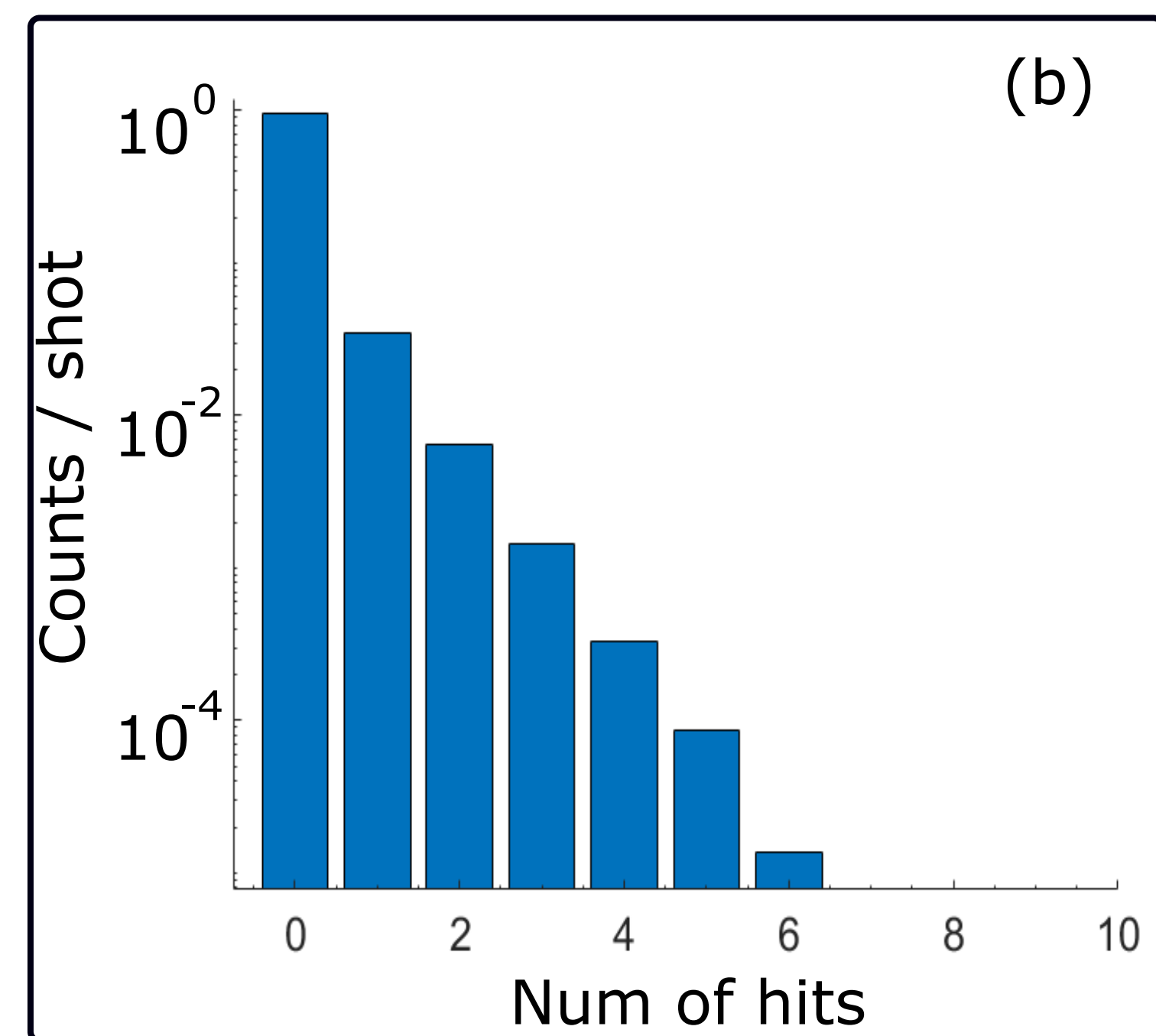
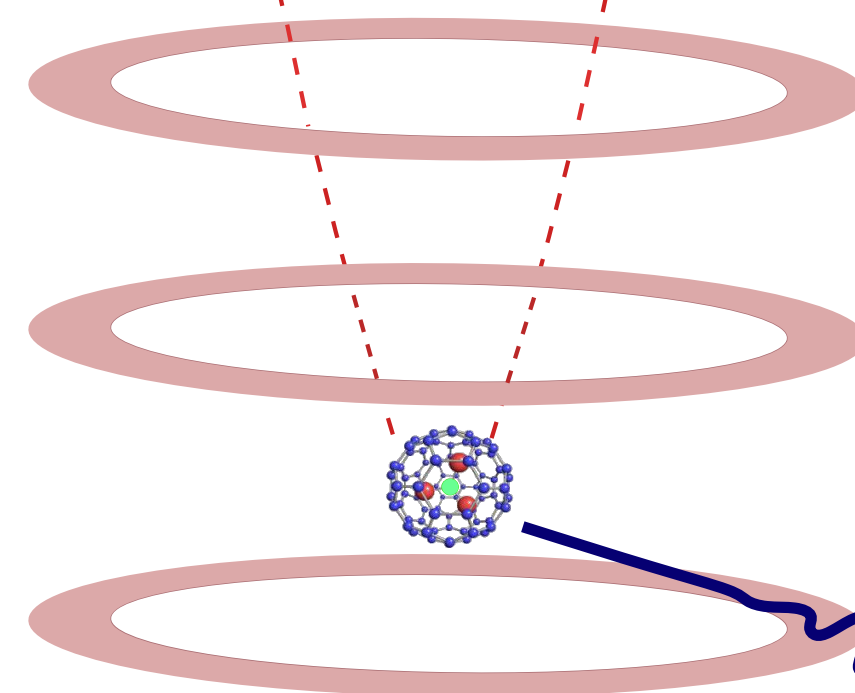
⁴⁰J. Hoszowska, A. Kheifets, J.-C. Dousse, M. Berset, I. Bray, W. Cao, K. Fennane, Y. Kayser, M. Kavčič, J. Szlachetko, *et al.*, “Physical mechanisms and scaling laws of K-shell double photoionization,” *Physical Review Letters* **102**, 073006 (2009).

- 41 E. B. Campbell, T. Raz, and R. Levine, "Internal energy dependence of the fragmentation
471 patterns of C_{60} and C_{60}^+ ," Chemical Physics Letters **253**, 261–267 (1996).
- 472 ⁴²H. Hohmann, R. Ehlich, S. Furrer, O. Kittelmann, J. Ringling, and E. E. B. Campbell,
473 "Photofragmentation of C_{60} ," Zeitschrift für Physik D Atoms, Molecules and Clusters **33**, 143–
474 151 (1995).
- 475 ⁴³Z. Jurek, B. Ziaja, and R. Santra, "Applicability of the classical molecular dynamics method to
476 study x-ray irradiated molecular systems," Journal of Physics B: Atomic, Molecular and Optical
477 Physics **47**, 124036 (2014).
- 478 ⁴⁴S. Cheng, H. Berry, R. Dunford, H. Esbensen, D. Gemmell, E. Kanter, T. LeBrun, and W. Bauer,
479 "Ionization and fragmentation of C_{60} by highly charged, high-energy xenon ions," Physical Re-
480 view A **54**, 3182 (1996).
- 481 ⁴⁵D. Gruyer, J. Frankland, R. Botet, M. Płoszajczak, E. Bonnet, A. Chbihi, G. Ademard,
482 M. Boisjoli, B. Borderie, R. Bougault, *et al.*, "Nuclear multifragmentation time scale and fluc-
483 tuations of the largest fragment size," Physical Review Letters **110**, 172701 (2013).
- 484 ⁴⁶A. Hirsch, A. Bujak, J. Finn, L. Gutay, R. Minich, N. Porile, R. Scharenberg, B. Stringfellow,
485 and F. Turkot, "Experimental results from high energy proton-nucleus interactions, critical phe-
486 nomena, and the thermal liquid drop model of fragment production," Physical Review C **29**, 508
487 (1984).



Oven dispensing $\text{Sc}_3\text{N@C}_{80}$

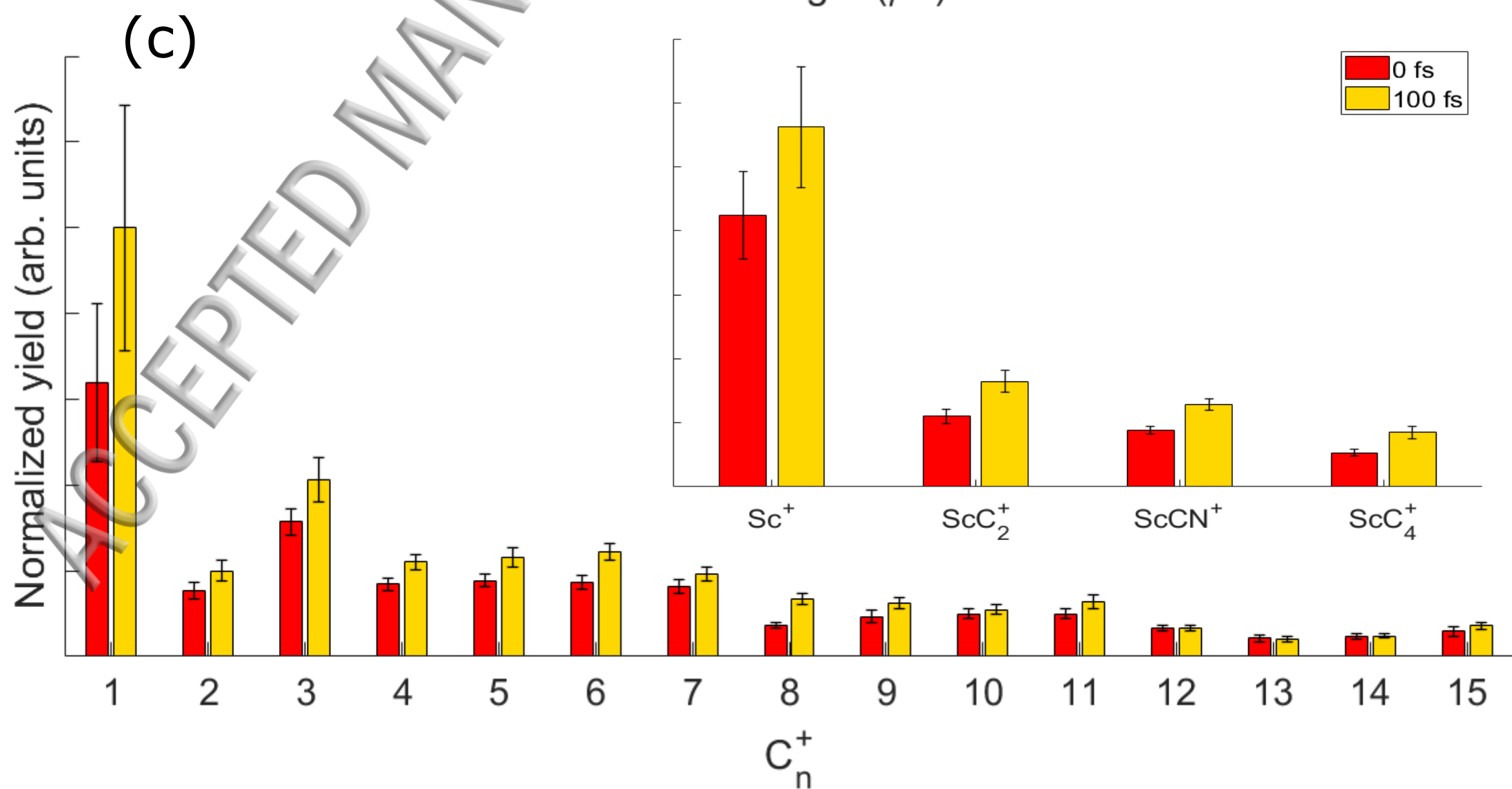
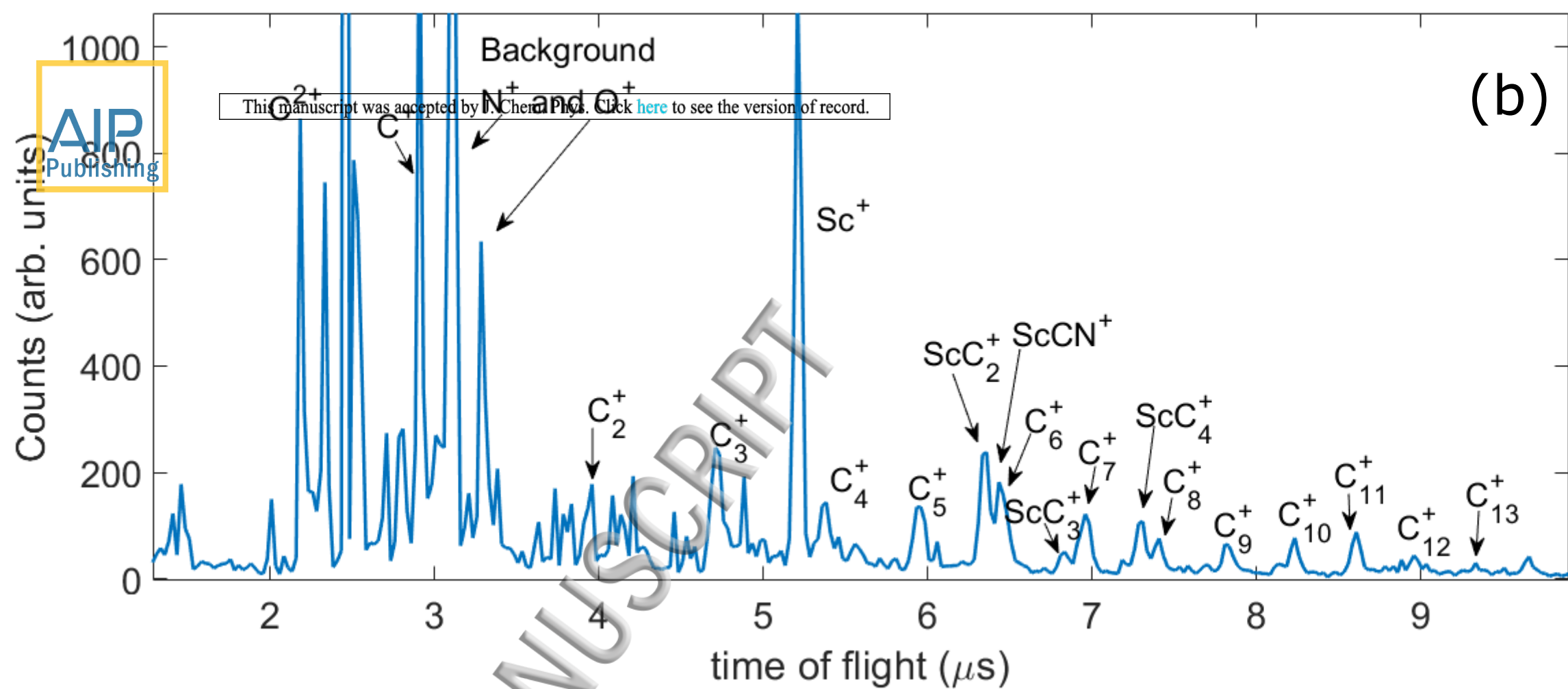
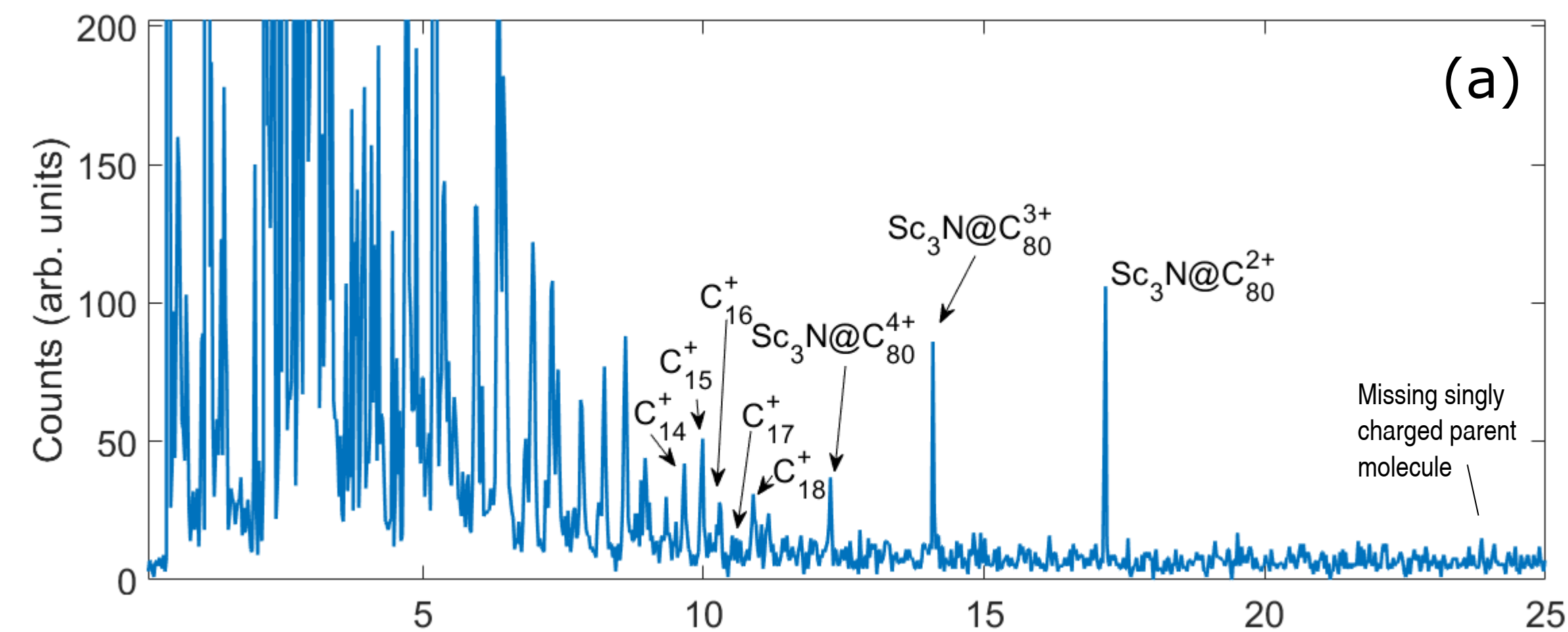
MCP for ion TOF



4.55 keV
FWHM = 13.11 eV

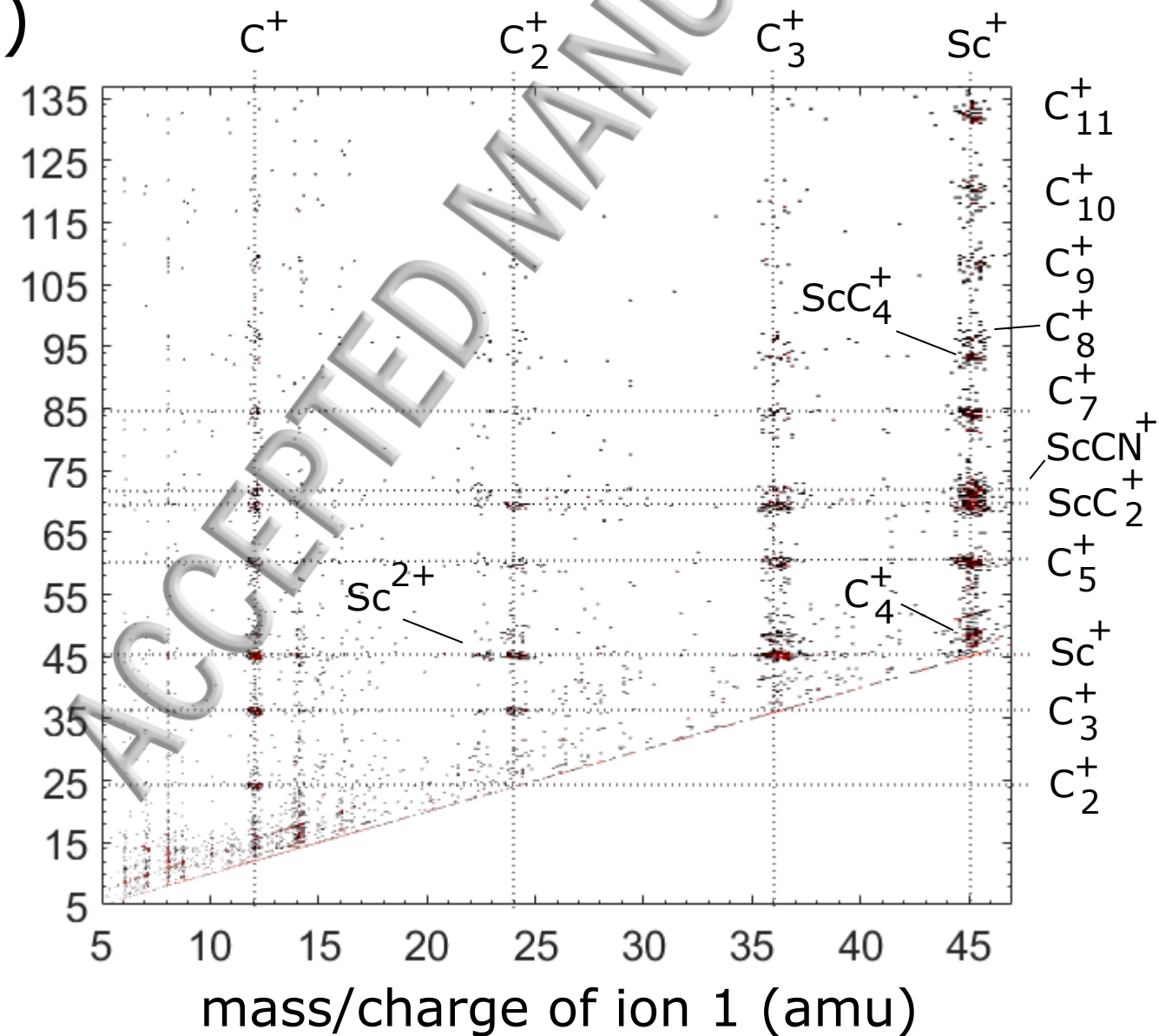
Pump and probe pulses with delays

5.0 keV
FWHM = 69.79 eV



(a)

mass/charge of ion 2 (amu)



(b)

Normalized yield (arb. units)

